

Effect of CdCl₂ Concentration and Heat Treatment on Electrodeposited Nano-Crystalline CdS Thin Films from Non-Aqueous Solution

Marwa Fathy^{1,*}, Abd El-Hady B. Kashyout¹, Shaimaa Elyamny¹, Gamal D. Roston²,
Ahmed A. Bishara²

¹Electronic Materials Research Department Advanced Technology and New Materials Research Institute, City of Scientific Research and Technological Applications (SRTA-City), New Borg El-Arab City, P.O. Box 21934, Alexandria, Egypt

²Department of physics, Faculty of science, Alexandria University, Egypt

*E-mail: mrwfathy@gmail.com

Received: 15 May 2014 / Accepted: 28 June 2014 / Published: 25 August 2014

Cadmium sulfide (CdS) window layers have been deposited on indium tin oxide (ITO)-coated glass substrates by electrodeposition using the galvanostatic method from non-aqueous solution containing cadmium chloride (CdCl₂), sulfur (S₈) and ammonium chloride (NH₄Cl) at bath temperature of 90 °C. Good quality CdS-deposited films are obtained at a cathodic current of 0.25 mA/cm². Structural, morphological, optical characterizations and electrical investigations have been carried out to determine the optimum CdCl₂ concentration and without or with heat treatment for the best CdS thin film properties. The X-ray diffraction showed that CdS films are polycrystalline in nature, with single hexagonal phase. Annealing the samples at 400 °C under oxygen atmosphere for 30 min resulted in an enhancement in crystallinity. Uniform, compact, free pinholes, stoichiometric, adherent, high optical transmittance and low resistivity CdS film is obtained using concentration of 0.2 M CdCl₂ in the bath deposition and after heat treatment.

Keywords: Nanocrystalline CdS; electrodeposition; non-aqueous; optical and electrical properties

1. INTRODUCTION

Cadmium sulfide (CdS) is a direct n-type semiconductor with a band gap of about 2.4 eV and large absorption coefficient of $4 \times 10^4 \text{ cm}^{-1}$ [1]. Deposition and characterization of transparent CdS on ITO glass substrates have been reported by many researchers. Research is still going on this material because of the potential applications in solar cell as windows materials including CdS/CdTe [2] and CdS/SnS solar cells [3], photocatalysis [4] and solid state optics [5].

The complete devices and individual layers of the devices are the subjects of processing/performance studies, which are sometimes empirical and sometimes present back tracking in order to establish the means by which they are effective [6].

A variety of deposition techniques have been reported in the literature for the preparation of CdS thin films; including sputtering [7], MOCVD [8], anodic oxidation, cathodic reduction, chemical vacuum deposition [9], spray pyrolysis [10,11], chemical bath deposition [12,13], successive ionic layer adsorption and reaction (SILAR) [14], electrochemical atomic layer epitaxy (ECALE) [15,16] or electrodeposition [17–19] from aqueous and non-aqueous solutions containing a soluble metal salt and sulfur compounds that has been developed. The latter method has drawn a special attention because of low cost, easy control of growth parameters and good adhesion of the obtained films to the substrate. Morphology and quality of the CdS films and, in consequence, efficiency of resultant photovoltaic cells, are strongly dependent on several parameters which should be very carefully adjusted: composition of the solution, especially sources and concentration of sulfur and cadmium ions [20–23], pH [20,24,25] and temperature [22,25–27] of electrodeposition bath as well as value of current density [28].

In this work, transparent CdS thin films on ITO glass substrates are electrodeposited using galvanostatic technique from non-aqueous solution bath consisting of Cadmium chloride, sulfur and ammonium chloride in ethylene glycol solution and the deposited films are annealed under oxygen atmosphere. Structural, morphological, optical and electronic properties are investigated to optimize the fabrication parameters to produce uniform, stable, adherent, stoichiometric, and conductive CdS thin films on ITO glass substrate.

2. EXPERIMENTAL

2.1. Methodology

The substrates are soda-lime glasses coated with Indium-Tin oxide thin film (ITO) layer using sputtering technique [29]. The overall thickness of ITO is about 650 nm. The substrate has high transparency and sheet resistance of about $12 \Omega/\square$. The substrates are cleaned in an ultrasonic bath with acetone, methanol and distilled water respectively. The substrates are taken out from the bath, and then dried under a stream of nitrogen [30]. ITO glass substrates are then etched for 30 sec in 0.1 M HCl at room temperature in order to remove impurities and increase the roughness of ITO surface, and finally washed in de-ionized water.

2.1.1. Preparation of CdS non-aqueous solution

Different concentrations of CdCl₂ ranged from 0.1 M to 0.3 M are added to 0.02 M of S₈ in ethylene glycol (non-aqueous solvent) due to its relative high boiling point (about 197.4 °C) as well as its stability at high temperatures [31]. Ammonium chloride is added with a concentration of 0.1 M, which plays an important factor as a supporting electrolyte and performs several functions in the

electrochemical process [32]. The solution temperature is adjusted at about 120 °C to dissolve S₈ and then is kept at about 90 °C with stirring rate of 300 rpm.

2.1.2. Electrodeposition of CdS thin films

A potentiogalvanostatic scan technique is used for the electrodeposition process. Good quality CdS films have been deposited using different concentration of CdCl₂ (as shown in Table 1) at current density of 0.25 mA/cm² for 1x1 cm² ITO glass substrate [29].

Table 1. Preparation parameters of CdS thin films

Samples	CdCl ₂ Concentration (M)	Sulfur Concentration (M)	NH ₄ Cl Concentration(M)	Annealing at 400 °C for 30 min
S1	0.1	0.02	0.1	-
S2	0.2	0.02	0.1	-
S3	0.3	0.02	0.1	-
S4	0.1	0.02	0.1	Annealed
S5	0.2	0.02	0.1	Annealed
S6	0.3	0.02	0.1	Annealed

Platinum sheet of size 2x2 cm² is used as the anode. The deposition bath temperature is 90 °C and a deposition time of 30 min to produce thin film thickness of 100 nm according to equation (1) [33].

$$d = JMt/nF\rho \quad (1)$$

Where d is the film thickness, J is the current density (mA/cm²), M is the molecular weight (g), t is the deposition time (sec), n is the number of electrons, F is Faraday constant (96500 C) and ρ is the CdS density (4.84 g/cm³).

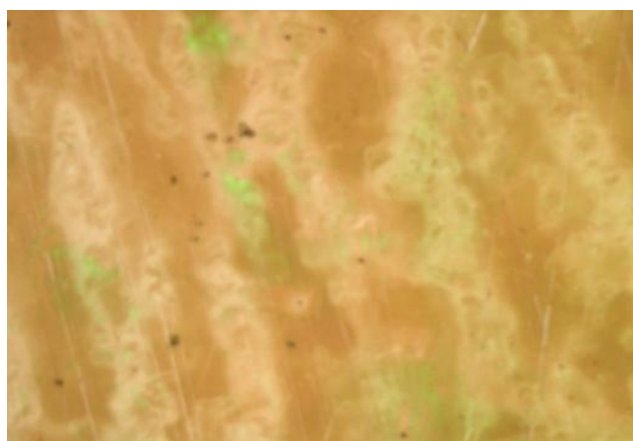


Figure 1. Optical microscope image of CdS thin film electrodeposited on ITO glass substrate at bath temperature of 100°C.

The effect of bath deposition temperature is studied in the literature, where as the deposition bath temperature increases, the grain size increases. Also the rise in temperature of the bath enhances the rate of diffusion, increases the ionic mobility and hence the conductivity of the bath. So the best deposition bath temperature is 90 °C because more homogenous crystallization is formed at this temperature [23]. So, below 90 °C, non uniform in nature, and above it, very thin visible cracks is produced [22], as shown in Figure 1.

The source used for sulfur ions is pure S₈ and the overall reaction is assumed to be [34].



This method has the advantage of being simple and needs only a power supply and a temperature controller to control the bath temperature during the deposition process. It has been demonstrated to be useful to avoid concentration gradients and precipitation. The obtained CdS films are homogeneous, smooth with a bright yellow color and good adhesion to the substrate. After deposition, the samples are rinsed in DI water and blown dry with filtered compressed air. The produced samples are annealed under oxygen atmosphere at 400°C for 30 min.

2.2. Characterization methods

X-ray powder diffraction measurements performed using Shimadzu 7000 XRD, with CuK_α radiation ($\lambda = 1.5418 \text{ \AA}$) generated at 30 kV and 30 mA with scanning rate of $4^{\circ} \text{ min}^{-1}$ for 2θ values between 20 and 70 degrees. The surfaces of the CdS thin films are investigated with high-resolution scanning electron microscopy (JEOL, JSM-6360 LA) to examine the morphology and the homogeneity of the surface. Thin films of gold are sputtered onto the samples to get charge free surfaces and an accelerated voltage of 30 kV is used. Composition of solid phases is estimated by energy dispersive spectrometry (EDS). Optical transmittance measurements are performed with double beam UV-Vis spectrophotometer under normal incidence in the range of 190 - 900 nm. The band gap energy (E_g) of CdS films is calculated using transmittance spectra.

Electrical properties of the films with thickness (t) of 0.8 μm are studied by Hall Effect measurement system (MMR Technologies, Inc.1400 North Shoreline Blvd., Unit A5, CA 94043). Resistivity, Sheet resistance R_s , mobility, Hall coefficient and type of carriers are measured by four prods. All measurements are made at room temperature.

3. RESULTS & DISCUSSION

3.1. Structural analysis

X-ray diffraction is used to analyze the formation of the crystalline phases. Generally, the hexagonal phase and the cubic phase are two crystalline modifications of CdS. X-ray diffraction (XRD) spectra of cadmium sulfide Samples; S1, S2, S3, S4, S5 and S6 are presented in Figure 2 as a function of the CdCl₂ concentration and heat treatment, respectively.

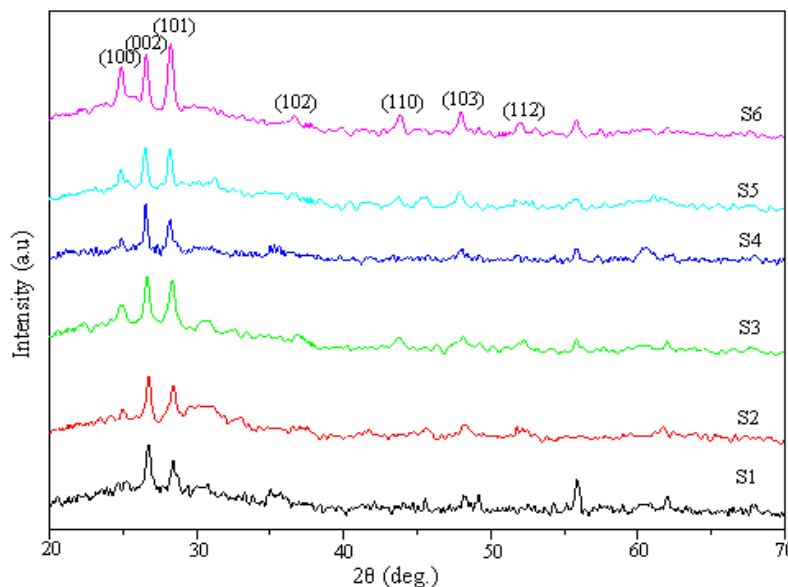


Figure 2. XRD spectra of electrodeposited CdS samples using different CdCl₂ concentrations, and before and after heat treatment.

For S1; the peaks at $2\theta = 26.45^\circ, 34.6^\circ$ are associated with a mixture of hexagonal (002)/cubic (111) planes [35] and the hexagonal (110)/cubic (220) planes of CdS, respectively. The peak at $2\theta = 24.8^\circ, 36.6^\circ, 47.8^\circ$ and 51.8° correspond to the hexagonal (102), (110), (103) and (112) planes, respectively (according to JCPDS card no. 41-1049) [36]. Beside these, no other peaks of cubic phase CdS appeared. Indicating that, the structure of the films is predominantly hexagonal which consider as the stable phase of CdS at room temperature [7]. For S2 and S3; the intensity of the peaks is increased which indicate that the crystallinity increased as the CdCl₂ concentration increase.

Table 2. Crystallite size, EDS analysis, and energy bandgap of CdS samples

Samples	Crystallite size (L) (nm)	Atomic ratio			E _g (eV)
		S	Cd	S/Cd	
S1	24	68.04	31.96	2.1	2.6
S2	30	56.88	43.12	1.3	2.43
S3	25	43.4	56.5	0.7	2.58
S4	34	65.11	34.89	1.8	2.497
S5	28	51.45	48.55	1.05	2.375
S6	29	45.13	54.87	0.8	2.543

For S4, S5, and S6, it is seen that no new peaks appeared, indicating that there are no new crystalline phases. However, the preferred orientation of heat treated CdS samples seems to be slightly

affected. The intensity of the peak increases and very slight shift towards lower scattering angles is observed. Increasing the peak intensity indicates improved crystallinity due to heat treatment process. The shift towards a lower and the consequent increase in the lattice parameter resulting in enlarging of the CdS lattice is due to the filling of the vacancies and the appearance of sulfur interstitial. Both defects contribute to the enlarging of the CdS cell [25]. Also, the position shift of the peaks may correspond to the relaxation of tensile stress [6] and recrystallization process [37].

The individual crystallite size (L) is determined using Scherrer's formula [38] (equation

$$L = k \cdot \lambda / B \cdot \cos \theta \quad (3)$$

where k is Scherrer's constant, which is a reference value corresponding to the quality factor of the apparatus measured with a reference single crystal and dependent on the crystallite shape (0.89–0.9). λ is the X-ray wave length, B is the FWHM (full width at half maximum) or integral breadth of the diffraction peak and θ is the Bragg angle [39]. The calculated data of the crystallite size are summarized in Table 2.

For CdS thin films, the crystallite size increased from 24 nm for S1 to 34 nm for S4 and increased from 25 nm for S3 to 29 nm for S6 as a result of heat treatment [39]. But for sample S2, there is a slight decrease in the crystallite size by heat treatment from 30 nm (S2) to 28 nm (S5).

3.1.2. Morphological analysis

Figure 3 Shows the SEM micrographs of CdS thin films grown on ITO/glass substrate using different CdCl₂ concentrations before and after heat treatment (S1, S2, and S3) and (S4, S5, and S6), respectively. Generally; CdS thin films grown on the ITO/glass substrates had a compact and regular structure having an average grain size of about 35 nm with very well define grain boundaries [30, 40, 41] as shown for S1, and S2. But for S3, with the increasing CdCl₂ concentration, CdS particles are aggregates and the grain sizes increased obviously. It is necessary to optimize the CdCl₂ concentration to obtain pore-free and compact CdS films. After heat treatment under oxygen atmosphere, there is no much difference, no pinholes and cracks among grain boundaries are observed, any oxide barriers can found on crystals are removed and the crystals are grown together [37] for S4 and S5 samples but S6 some particles are found on the surface of the CdS film and grains coalesce between them producing larger sizes and holes which is also observed in the other reports [8].

EDS analysis of all CdS samples is summarized in Table 2. It confirms that the composition of cadmium and sulfur in CdS films on ITO/glass substrate is related to the CdCl₂ concentration. S1, the S/Cd atomic ratio is 2.1, which indicates free sulfur content. Increasing the Cd concentration to 0.2 M and maintaining S ions as 0.02 M, S/Cd ratio becomes 1.3, which approximated to the stoichiometric ratio [7]. By further increasing the Cd concentration to 0.3 M, S/Cd ratio is reduced to 0.76 due to produce Cd rich sample.

After heat treatment under oxygen atmosphere, sulphur deficiency is observed in all the films. This may be due to the fact that sulphur has great affinity towards oxygen, so it might have converted to SO₂ and then evaporated. EDS result of S5 reveals that the deposited films are very close to the nominal composition [42].

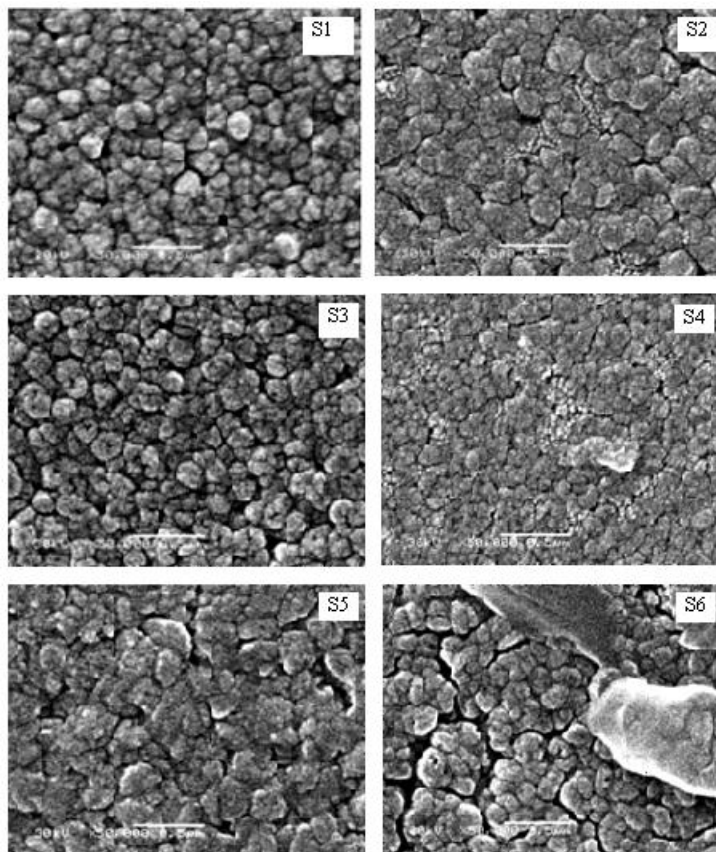


Figure 3. SEM images of electrodeposited CdS thin films samples.

3.1.3. Optical and electrical analysis

The Transmittance spectra of as-deposited and heat treated CdS samples are studied at normal incidence in the wave length range from 300 to 900 nm, as shown in Figure 4.

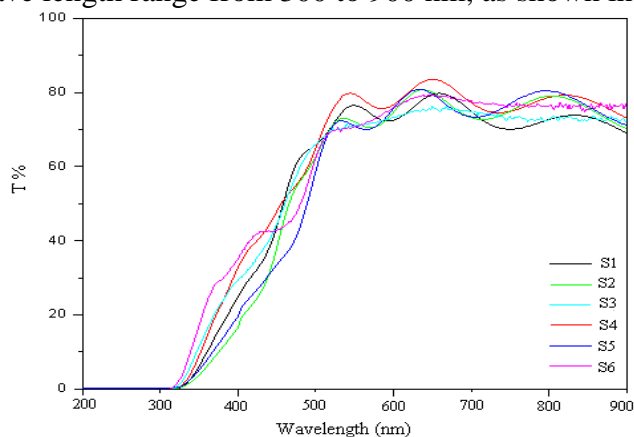


Figure 4. Optical transmittance spectra of CdS thin film samples.

The spectra exhibited interference fringes and the value of refractive index is estimated by the envelop method as follows [43, 44]:

$$\alpha = \frac{1}{d} \ln \left\{ \frac{(n - 1)(n - n_s)}{(n + 1)(n + n_s)} \left[\left(\frac{T_{max}}{T_{min}} \right)^2 + 1 \right] / \left[\left(\frac{T_{max}}{T_{min}} \right)^2 - 1 \right] \right\} \quad (4)$$

$$d = \frac{\lambda_1 \lambda_2}{2n(\lambda_2 - \lambda_1)} \quad (5)$$

$$n = \frac{N + (N^2 - n_s^2)^{1/2}}{2} \quad (6)$$

$$N = \frac{(n_s^2 + 1)/2 + 2n_s(T_{max} - T_{min})/T_{max} T_{min}}{2} \quad (7)$$

Where n and n_s are the refractive index of the sample and the substrate, respectively, T_{max} , T_{min} are the maximum and minimum transmittances at the same wavelength in the fitted envelope curve on a transmittance spectrum, α is the absorption coefficient, d is the film thickness, λ_1 and λ_2 are the wavelengths at the two adjacent maxima or minima. The absorption coefficient for the direct allowed transition can be described as a function of photon energy [45] as equation (8).

$$\alpha \approx A (h\nu - E_g)^2 \quad (8)$$

Where A is the constant which is related to the effective masses associated with the bands, ν is the frequency of the incident photons and $h\nu$ is the photon energy [46].

For as deposited samples (S1, S2 and S3), the average transmittance of the films on ITO/glass substrates is about 76, 77, and 74%, and the E_g is 2.6, 2.43, and 2.58 eV (as shown in Table 2), respectively. The higher transmittance (S1 and S2) indicates lower defect density and better electrical properties of the CdS films because the absorption of light in the wavelength longer region is usually caused by crystalline defects such as grain boundaries and dislocations [7] but S3 exhibits lower transmission because it is cadmium rich, also no fringes observed which indicate low film adhesion on ITO/glass substrate.

After heat treatment, the optical transmission for S4, S5, and S6 increases and the absorption edge becomes much sharper. This is due to improve the crystallinity of the samples. Also, a decrease of the band gap of S4, S5 and S6 to 2.49, 2.37, and 2.54eV, respectively is observed as reported previously by other authors [25]. This may be due to electron-electron and electron impurity interaction.

The electrical properties of the CdS films are examined at room temperature by resistivity and Hall measurements using Van der Pauw method and summarized in Table 3.

Table 3. The electrical properties of CdS thin films.

Samples	Resistivity ($\Omega \cdot \text{cm}$)	Mobility (cm^2/Vs)	Carriers Density (cm^{-3})	Hall coefficient ($\text{cm}^3/\text{coul.}$)	Sheet resistance (Ω/cm^2)
S1	2.3	6.79×10^{-5}	3.97×10^{12}	1.57×10^6	4.6×10^4
S2	6.6×10^{-1}	2×10^2	4.67×10^{16}	1.335×10^2	8.29×10^3
S3	2.2×10^{-1}	5.45×10^3	5.1×10^{15}	1.2×10^3	2.77×10^3
S4	3.67	2.01×10^3	8.46×10^{13}	7.38×10^3	7.33×10^4
S5	2.31	4.5×10^3	6×10^{14}	1.04×10^4	2.89×10^4
S6	2.2×10	1.18×10^3	2.37×10^{13}	2.63×10^5	2.28×10^5

It is observed that, for S1, S2, and S3 samples, the resistivity decreases and Hall mobility increases with CdCl₂ concentration increases. This may be due to the change in film stoichiometry (excess cadmium or sulphur vacancies, which are electron donor sites that provide the additional carriers and decrease the resistivity) [47].

The conduction of CdS films at room temperature can also be explained considering the micro-structural aspects. S2 has higher carrier concentration than another two samples. Consequently; S2 has lower sheet resistance than S1 which strongly depends on the variations in charge-carrier density rather than the mobility. The density of the major carriers of the CdS film can be relatively calculated from the following relation [48, 49].

$$N = 1/(e \times R_H) \quad (9)$$

Where N is the density of the majority carriers, e is the Charge of the electron, and R_H is the hall coefficient [50].

Also, the grain boundaries between the crystallites dominate the electrical properties of the polycrystalline thin film semiconductors [51]. Carrier traps at the grain boundaries are responsible for the potential barrier that limits carrier mobility.

The carrier mobility is inversely proportional to the film roughness and the carrier concentration is proportional to the grain size [52]. Experimentally; the type of CdS film is found as n-type, depending on the value of Hall Factor (R_H) which is calculated by using the equation:

$$R_H = (V_H \times t)/(I \times B) \quad (10)$$

R_H is measured for the film at B = 0.1 Tesla. Where; I is the current flow through the film, V_H is the generated voltage on both sides of the film, and B is the magnetic field.

The influence of heat treatment process on the resistivity of the films is depicted in Table 3. The magnitude of the resistivity increased with heat treatment for all samples. It is attributed to the change in film stoichiometry (excess of sulfur vacancies which are electron donor sites that provide the additional carriers and decrease the resistivity). In addition, during the heat treatment process, oxygen fills the S vacancies so the donor sites are eliminated, the free carrier concentration is reduced as shown in table. The absorbed oxygen offsets the decrease in resistivity due to the excess carriers provided by the excess cadmium obtained on heat treatment resulting in a net increase of resistivity [47].

The carrier mobility increases for S4 and S5 samples from 6.79 × 10⁻⁵ to 2.01 × 10³(cm²/N_s), and from 2 × 10² to 4.5 × 10³(cm²/N_s), respectively. It is attributed to, after heat treatment, the crystals are grown together and the electrical contacts between them are improved [37]. But for S6, The grain boundaries between crystals dominate the electrical properties of the sample. Traps at grain boundaries are responsible for the potential barrier that limits carrier mobility [47].

4. CONCLUSIONS

The structural, morphological, optical and electrical properties of CdS film electrodeposited on ITO glass substrate from non-aqueous solution as a function of different CdCl₂ concentrations and heat treatment in oxygen atmosphere are investigated. XRD patterns indicated that the structure of CdS film

is hexagonal and the crystallinity increased after heat treatment under oxygen atmosphere. The as prepared CdS film using 0.2 M CdCl₂, 0.02 M S₈, and 0.01M NH₄Cl is uniform, compact and free of holes and after heat treatment, the grain sizes of the film are almost the same as the deposited film and no pinholes and cracks among the grain boundaries are observed. Increasing CdCl₂ concentration in the deposition bath and heat treatment also make some effect on the optical transmittance of the CdS films and the optical bandgap of the film. The film stoichiometry plays an important role in the resistivity of the CdS film. During the heat treatment under oxygen atmosphere, the oxygen fills the S vacancies in the CdS and the doner sites are eliminated which effect the reduction in the carrier concentration and consequently the resistivity is increased.

ACKNOWLEDGEMENT

A part of this work has been supported by the Ministry of Science Research (ASRT), Egypt, under the Science and Technology Development Fund Program (STDF). Project ID: 1396 with title "Synthesis of thin films to produce photovoltaic solar cells".

References

1. K. Senthil, D. Mangalaraj, Sa. K. Narayandass, B. Hong, Y. Roh, C.S. Park, J. Yi, *Semicond. Sci. Technol.* 17 (2002) 97 - 103.
2. M. Soliman, A. B. Kashyout, M. El-Gamal, M. Shabana, 17th European Solar Energy Conference, (2001).
3. J. Xu, Y. Yang, *Energy Conversion and Management*, 78 (2014) 260-265.
4. H. Zhang, G. Chen, D.W. Bahnemann, *J. Mater. Chem.* 19 (2009) 5089-5121.
5. Y. Wang, Z. Tang, M.A. Correa-Duarte, L.M. Liz-Marzan, N.A. Kotov, *J. Am. Chem. Soc.* 125 (2003) 2830-2831.
6. M.K. Al Turkestani, K. Durose, *Sol. Energy Mater. Sol. Cells*, 95 (2011) 491-496.
7. M. Cao, L. Li, B.L. Zhang, J. Huang, K. Tang, H. Cao, Y. Sun, Y. Shen, *J. Alloys and Compounds* 530 (2012) 81-84.
8. J. Han, C. Liao, T. Jiang, G. Fu, V. Krishnakumar, C. Spanheimer, G. Haindl, Kui Zhao, A. Klein, W. Jaegermann, *Mater. Res. Bull.* 46 (2011) 194 -198.
9. N.I. Fainer, M.L. Kosinova, Yu.M. Rumyantsev, E.G. Salman, F.A. Kuznetsov, *Thin Solid Films* 280 (1996) 16 - 19.
10. S. Mathew, P.S. Mukerjee, K.P. Vijayakumar, *Thin Solid Films* 254 (1995) 278 - 284.
11. J. Hiie, T. Dedova, V. Valdna, K. Muska, *Thin Solid Films* 511-512 (2006) 443 - 447.
12. J.P. Enriquez, X. Mathew, *Sol. Energy Mater. Sol. Cells* 76 (2003) 313- 322.
13. R.S. Mane, C.D. Lokhande, *Mater. Chem. Phys.* 65 (2000) 1- 31.
14. B.R. Sankapal, R.S. Mane, C.D. Lokhande, *Mater. Res. Bull.* 35 (2000) 177 - 184.
15. B.W. Gregory, J.L. Stickney, *J. Electroanal. Chem.* 300 (1991) 543 - 561.
16. M. Innocenti, S. Cattarin, M. Cavallini, F. Loglio, M.L. Foresti, *J. Electroanal. Chem.* 532 (2002) 219 - 225.
17. I. Sisman, M. Alanyahoglu, U. Demir, *J. Phys. Chem. C* 111 (2007) 2670 - 2674.
18. D. Lincot, *Thin Solid Films*, 487 (2005) 40 - 48.
19. M. Bouroushian, Ed. F. Scholz, *Electrochemistry of Metal Chalcogenides*, Springer, Verlag Berlin Heidelberg (2010) 91.

20. J. Nishino, S. Chatani, Y. Uotani, Y. Nosaka, *J. Electroanal. Chem.* 473 (1999) 217 - 222.
21. M. Takahashi, S. Hasegawa, M. Watanabe, T. Miyuki, S. Ikeda, K. Iida, *J. Appl. Electrochem.* 32 (2002) 359-367.
22. S.J. Lade, C.D. Lokhande, *Mater. Chem. Phys.* 49 (1997) 160.
23. F. Kadirgan, D. Mao, W. Song, T. Ohno, B. McCandless, *Turk. J. Chem.* 24 (2000) 21- 33.
24. G.P. Power, D.R. Peggs, A.J. Parker, *Electrochim. Acta* 26 (1981) 681- 682.
25. G. Sasikala, R. Dhanasekaran, C. Subramanian, *Thin Solid Films* 302 (1997) 71- 76.
26. S. Dennison, *Electrochim. Acta* 38 (1993) 2395- 2403.
27. S. J. Lade, M.D. Uplane, C.D. Lokhande, *Mater. Chem. Phys.* 53 (1998) 239 - 242.
28. B.E. McCandless, A. Mondal, R.W. Birkmire, *Sol. Energy Mater. Sol. Cells* 36 (1995) 369 - 379.
29. A.B. Kashyout, M. Fathy, M. B. Soliman, *International J. Photoenergy*, Article ID 139374 (2011) 1-6.
30. M. Rami, E. Benamar, M. Fahoume, A. Ennaoui, *Physica Status Solidi* 172 (1999) 137 - 147.
31. R. K. Pandey, S. N. Sahu, S. Chandra, Hand book of semiconductor electrodeposition, Marcel Dekker Inc., New York (1996) 95.
32. A. B. Kashyout, M.M. Shabana, M.A. El-Gamal, M. B. Soliman, The effect of preparation parameters on the properties of CdTe films thesis, Alexandria university (2001) 66.
33. O.A. Ileperuma, C. Vithana, K. Premaratne, S.N. Akurathilaka, S.M. MCGregor, I.M. Dharmadasa, *J. Materials Science: Materials in electronics*, 9 (1998) 367-372.
34. W.J. Danaher, L.E. Lyons, G.C. Morris, *Sol. Energy Mater. Sol. Cells*, 12 (1985)137-148.
35. S. Butt, N. A. Shah, A. Nazir, Z. Ali, A. Maqsood, *J. Alloys and Compounds*, 587 (2014) 582–587.
36. H.Kim, D. Kim, *Sol. Energy Mater. Sol. Cells*, 67 (2001) 297-304.
37. J. Hiie, K. Muska, V. Valdna, V. Mikli, A. Taklaja, A. Gavrilov, *Thin solid films*, 516 (2008) 7008-7012.
38. B. D. Cullity, Elements of X-Ray Diffraction, 2nd ed. Addison Wesley, U.S.A. (1978) Chap. 3, 102.
39. S. Chun, K.S. Han, J.S. Lee, H.J. Lim, H. Lee, D. Kim, *Current Applied Physics*, 10 (2010) S196–S200.
40. J. Hernández-Borja, Y.V. Vorobiev , R. Ramirez-Bon, *Sol. Energy Mater. Sol. Cells*, 95 (2011) 1882–1888.
41. J.-H. Lee, *Thin Solid Films*, 515 (2007) 6089–6093.
42. A. Hasnat, J. Podder, *J. Bangladesh Academy of Sciences*, 37 (2013) 33-41.
43. M. Miyake, K. Murase, T. Hirato, Y. Awakura, *J. Electroanal. Chem.*, 562 (2004) 247 - 253.
44. M. Miyake, K. Murase, T. Hirato, Y. Awakura, *J. Electrochem. Soc.*, 150 (2003) C413.
45. J. Herrero and C. Guillen, *J. Appl. Phys.*, 69 (1991) 429 - 434.
46. E. Fatas, P. Herrasti, T. Garcia, *Materials Chemistry and Physics*, 13 (1985) 497 - 502.
47. K.R. Murali, M. Matheline, R. John, *Chalcogenide Letters* 6 (2009) 483 – 490.
48. R. Hill, Ed. T. J. Coutts, Active and passive thin film devices, Academic press, New York (1978).
49. J. I. B. Wilson, J. Woods, *J. Physics and Chemistry of Solids*, 34 (1973) 171-181.
50. A. M. Suhail, W. A. A. Twej , S. S. Abdulah, N. M. Saeed, IBN AL- HAITHAM J. FOR PURE & APPL. SCI, 22 (2009) 2 - 10.
51. L.L. Kazmerski, Polycrystalline and amorphous thin film devices, Academic press, New York (1980).
52. W. C. Shin and S. G. Yoon, *J. Electrochem. Soc.* 144 (1997) 1055 - 1060.